

Full Paper

Design and Discovery of Some Novel Chalcones as Antioxidant and Anti-Inflammatory Agents via Attenuating NF- κ B

Jun Chu and Chun-Liang Guo

Department of Hepatobiliary Surgery, Affiliated Hospital of Logistics University of PAPF, Tianjin, P. R. China

Concerning the role of antioxidant and anti-inflammatory agents for hepatic fibrosis patients, the current study deals with the development of novel chalcone derivatives **5a–i** via efficient synthetic methodology in a two-step reaction involving Claisen–Schmidt condensation. The obtained target analogs were screened for *in vitro* antioxidant activity by various methods (H_2O_2 , DPPH, ferrous reducing power, and nitric oxide), where they exhibit considerable radical scavenging activity. These compounds were also evaluated for inhibitory potency against NF- κ B activation induced by LPS for the determination of their anti-inflammatory activity. The inhibition values indicate that the entire set of compounds efficiently inhibits the NF- κ B activation provoked by LPS. Among the series, compound **5i** was identified as the most potent inhibitor of NF- κ B, with a relative NF- κ B activity of 1.12 ± 0.53 . It also inhibits various inflammatory mediators, such as TNF- α , IL-1 β , IL-6, and PGE₂.

Keywords: Anti-inflammatory / Antioxidant / Chalcones / Hepatic fibrosis

Received: September 24, 2015; Revised: November 16, 2015; Accepted: November 20, 2015

DOI 10.1002/ardp.201500349



Additional supporting information may be found in the online version of this article at the publisher's web-site.

Introduction

The liver is a vital organ of the body necessary for performing critical functions to maintain homeostasis and health. It executes tasks related to digestion, metabolism, immunity, storage of nutrients within the body and detoxification and degradation of foreign (e.g., drugs) and naturally occurring chemicals [1]. Thus, improper functioning of liver due to these four diseases, like cirrhosis, fatty liver, hepatitis, and liver cancer can sternly have an effect on health and can be life threatening. Out of them, hepatic fibrosis patients are prone to serious complications by almost all systems, leading to high morbidity rates and even death because of liver cirrhosis and hepatic failure [2, 3]. At the molecular level, it includes hepatocyte damage, Kupffer cell activation, hepatic stellate

cell (HSC) activation, and proliferation whereas, the hepatocyte, Kupffer cell, and HSC communicate through oxygen stress, which causes inhibition of electron transport, increasing ROS production, and decreasing mitochondrial glutathione [4]. Thus, the use of antioxidants diminishes fibrosis and HSCs, by halting the associated cell communication [5].

On the other hand, the studies concluded that chronic inflammation of the liver is the key component to initiate fibrosis by the infiltration and activation of immune cells [6]. This will in turn initiate both inflammatory and wound healing responses, including subsequent necrosis and apoptosis of parenchymal cells and replacement by connective tissue and extracellular matrix (ECM) proteins. According to recent studies, it has been suggested that activation of the proinflammatory nuclear factor- κ B (NF- κ B) pathway in hepatocytes is a key factor responsible for inflammation of fibrotic liver [7]. The family of NF- κ B transcription factors belongs to the key regulators of inflammatory processes. Therefore, aberrant activation of NF- κ B can lead to constitutive overproduction of proinflammatory cytokines, which is associated with a number of chronic inflammatory disorders as seen in the case of patients with liver diseases such as hepatitis B, hepatitis C, or hepatocellular carcinoma [8].

Correspondence: Dr. Jun Chu, Department of Hepatobiliary Surgery, Affiliated Hospital of Logistics University of PAPF, No. 220 Chenglin Road, Hedong District 300162, Tianjin, P. R. China.
E-mail: junchuchai@hotmail.com
Fax: +86 022 60578778

Concerning the above, dual targeting of drugs on inflammatory cascade and production of ROS species could contribute the beneficial and much more pronounced effect than individual drug alone.

In this regard, chalcones, a β -ketone scaffold developed via Claisen–Schmidt condensation [9] reaction between aromatic aldehydes and ketone have proved to exhibit numerous pharmacological activities ranging from anticancer [10], antibacterial [11], antifungal [12], anti-HIV [13], antimalarial [14], and other. More specifically, these chalcones are also proved to exhibit antioxidant and anti-inflammatory activities [15, 16]. Thus, in extension of this, we wish to report the development of novel series of chalcones substituted with numerous groups and tested for antioxidant and anti-inflammatory properties.

Results and discussion

Chemistry

The synthesis of the target compounds was achieved in two-step reaction as depicted in Scheme 1. Initially, the synthesis of *N*-(3-acetylphenyl)-4-fluorobenzamide (**3**) was achieved by reaction between 1-(3-amino-phenyl)ethanone (**1**) and 4-fluorobenzoyl chloride (**2**) via nucleophilic reaction in the presence of activating base NaOH. The furnished product (**3**) was then allowed to react with substituted aromatic aldehyde (**4**) to afford the corresponding chalcone derivatives (**5a–i**) via Claisen–Schmidt condensation. The target compounds were obtained in excellent yields and their structures were ascertained on the basis of various spectroscopic and analytical techniques.

The melting points of the all synthesized compounds **5a–i** and their ^1H NMR and ^{13}C NMR data along with the elemental analysis (percentage C, H, and N analysis) and mass analysis are given in the Experimental section. FT-IR spectra of the synthesized compound clearly show C–H stretching absorption bands at 3066 cm^{-1} due to aromatic ring and C=O stretching absorption bands at around 1718 cm^{-1} , respectively. Compound **5i** has also showed strong absorption band

around 1612 cm^{-1} which is attributable aromatic C=C bonds. The N–H bond was confirmed by the presence of absorption bands around at 3498 cm^{-1} . The absorptions at 786 and 868 cm^{-1} were characterized for the F and Cl groups. In ^1H NMR spectra, the characteristic shift corresponds to N–H and aliphatic C–H of side chain was observed around at 9.14–9.17 and 8.12–8.15 ppm, respectively. The chemical shift of aromatic hydrocarbon was seen at 8.11–7.42 ppm. The singlet at 5.38 ppm for proton was attributable to an aromatic hydroxyl group. The ^{13}C NMR shift of all final compounds was observed in the expected region. Finally, all the structures of title compounds were confirmed by mass and elemental analyses.

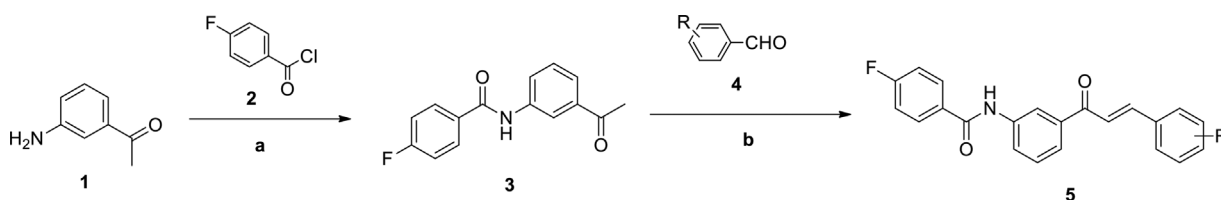
Biological activity

In vitro antioxidant activity

As seen in Table 1, the entire set of target analogs was assessed for antioxidant activity in various *in vitro* methods. All the synthesized compounds showed considerable activity ranging from mild to moderate against hydrogen peroxide. The results revealed compound **5a** as most potent derivative and exhibited 93.82% of inhibition. This was followed by decrease in activity for its isomeric congeners. The same pattern of percentage of inhibition was revealed for next analogs, i.e., **5d**, **5e**, and **5f**. However, a marked increase in activity was reported by compound **5i**, whereas rest of the compounds showed mild inhibition of H_2O_2 scavenging activity.

In the case of DPPH free radical scavenging activity, compounds **5i**, **5c**, and **5a** were identified as most potent and showed excellent activity than standard ascorbic acid whereas the rest of compounds exhibited mild to moderate scavenging activity. For determination of ferrous reducing ability of compounds, among the series, except compounds **5g**, **5h**, and **5i** entire set of analogs showed excellent reducing power than standard.

The nitric oxide radical scavenging activity result revealed that all the synthesized derivatives showed excellent activity than standard ascorbic acid. Among the series, in the inhibitory assay, compound **5a** was revealed as the most potent analog and **5h** as least potent.



Where R

5a = 4-OH	5d = 4-OCH ₃	5g = 4-Cl
5b = 3-OH	5e = 3-OCH ₃	5h = 4-Br
5c = 2-OH	5f = 2-OCH ₃	5i = 4-F

Scheme 1. Synthesis of compounds **5a–i**. (a) 5% NaOH; (b) ethanol, aq. NaOH.

Table 1. Antioxidant activity of target analogs.

Entry	H ₂ O ₂	DPPH	Ferrous reducing power	Nitric oxide radical scavenging activity
5a	93.82	45.76	56.96	76.33
5b	84.56	51.34	55.16	71.67
5c	83.44	54.56	50.71	73.17
5d	66.43	40.87	43.54	61.15
5e	63.28	40.94	48.36	56.42
5f	60.69	35.18	41.59	55.87
5g	32.14	33.56	38.42	45.61
5h	28.94	28.13	35.82	39.19
5i	63.35	51.35	39.04	44.84
BHT	86.36	–	–	–
Ascorbic acid	–	43.54	40.87	35.76

NF-κB inhibition assay

The target compounds **5a–i** assayed their inhibitory potency against NF-κB activation induced by LPS. The results of assay are summarized in Table 2. The inhibition values indicate that the entire set of compounds efficiently inhibits the NF-κB activation provoked by LPS. Compounds **5a**, **5b**, and **5c**, containing an isomeric hydroxyl group showed mild inhibitory activity, and out of which, *meta*-substituted derivative was found most active. In the next instance, compounds containing the methoxy group at various positions on the phenyl exhibit mild to moderate activity. Moreover, among the synthesized chalcone derivatives, compound **5i** was proved as the most efficient inhibitor of NF-κB. The minor decline in activity was reported by compounds **5g** and **5h** containing halogen electron withdrawing group. It was revealed that the inhibitory activity of the compounds was greatly influenced by the nature of the substituent and their position. In the study, the control group was calculated without stimulating by LPS (with the relative NF-κB activity (NF-κB/TK, fold): 1.53 ± 0.52) whereas, the LPS group was defined as the

stimulated group (with the relative NF-κB activity (NF-κB/TK, fold): 5.75 ± 1.63). Structure–activity relationships (SAR) of novel chalcone derivatives demonstrated that compounds with *para* electron-withdrawing substituents (**5g–i**) showed more potent activities than those with electron-donating substituents (**5a–f**). Whereas, compounds having *para*, *ortho*, and *meta* substituents on the aromatic ring demonstrated that an electron-donating group (**5d–f**) slightly improved the NF-κB inhibitory activity with the order of potency being $4\text{-OCH}_3 > 2\text{-OCH}_3 > 3\text{-OCH}_3$. Moreover, in the case of compounds (**5g–i**) with a halogen atom on the 4-position of aromatic ring, the order of inhibitory activity is $\text{F} > \text{Br} > \text{Cl}$.

Cell viability

To assess the effect of compound **5i** on the viability of cells, it has been tested against the RAW264.7 cells via MTT assay. As shown in Fig. 1, it was indicated that compound **5i** did not induce any loss of cell viability even at the higher tested concentration of 50 μg/mL. Thus, it could be suggested that compound **5i** was found non-toxic to macrophages and its

Table 2. Effect of target compounds on NF-κB transcriptional activity in LPS-stimulated RAW264.7 cells.

Analog	Relative NF-κB activity (NF-κB/TK, fold)
5a	3.85 ± 1.62^a
5b	4.66 ± 1.43^a
5c	4.01 ± 1.45^a
5d	3.12 ± 0.39^a
5e	4.76 ± 1.25^a
5f	3.73 ± 1.11^a
5g	3.76 ± 0.32^a
5h	2.14 ± 0.34^a
5i	1.12 ± 0.53^a
Control	1.53 ± 0.52
LPS	5.75 ± 1.63^b

N = 3.

^{a)} *p* < 0.01 versus LPS.

^{b)} *p* < 0.01 versus control.

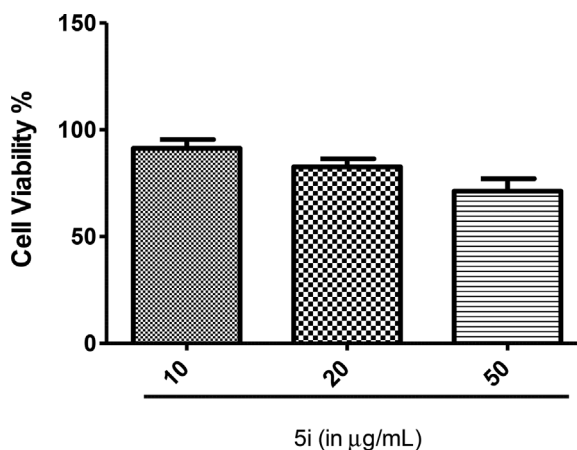


Figure 1. Effect of compound **5i** on the viability of RAW264.5 cells.

NF- κ B inhibition is entirely dependent on the ability to exert pharmacological effect.

Effect of compound 5i on pro-inflammatory mediators

To explain the inhibitory effect of the compound 5i on the production of inflammatory mediators, various immunoassays were conducted for TNF- α , IL-1 β , IL-6, and PGE₂. In the current study, RAW264.7 cells were treated with different concentrations of compound 5i for 1 h before the treatment of cells with 1 μ g/mL of lipopolysaccharide to stimulate inflammatory process. After 1 day of incubation, inured media were collected, and then the level of inflammatory mediators was measured. As shown in Figs. 2–5, compound 5i

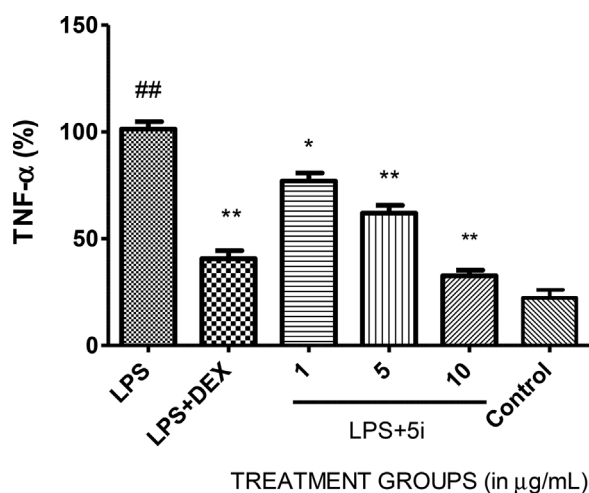


Figure 2. Effect of compound 5i on TNF- α . The values presented are mean \pm SEM. ## p < 0.01 versus control, * p < 0.05, ** p < 0.01 versus LPS.

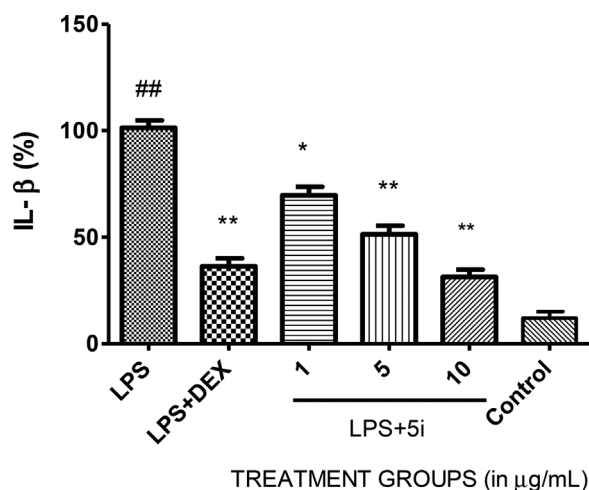


Figure 3. Effect of compound 5i on IL- β . The values presented are mean \pm SEM. ## p < 0.01 versus control, * p < 0.05, ** p < 0.01 versus LPS.

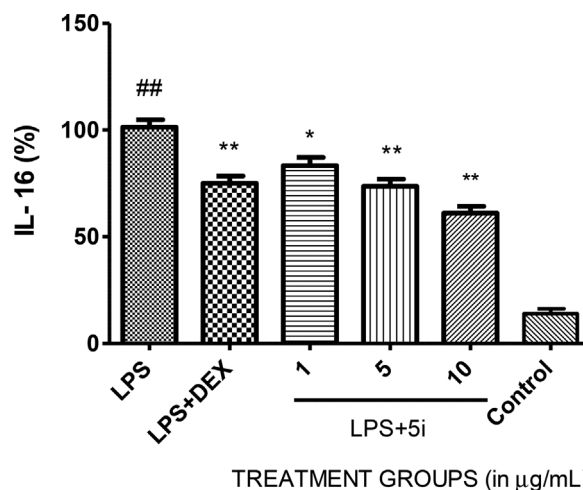


Figure 4. Effect of compound 5i on IL-16. The values presented are mean \pm SEM. ## p < 0.01 versus control, * p < 0.05, ** p < 0.01 versus LPS.

exhibited a dose-dependent inhibitory effect on the production of all inflammatory mediators. The 10 μ g/mL of compound 5i decreased TNF- α level as compared to blank group (Fig. 2). Moreover, It has been found that no significant difference in inhibitory potency was observed against TNF- α between dexamethasone at 1 μ M and treatment group of 5i above 5 μ g/mL. As shown in Fig. 3, the inhibitory effect of 5i on the production of IL-1 β was remarkably compared with those of other cytokines whereas, it was surprising to note that the level of IL-6 in the presence of 5i at 10 μ M was comparable to that of dexamethasone at 1 μ M (Fig. 4). The inhibitory effect of 5i on production of PGE₂ was more pronounced than those on the production of cytokines (Fig. 5). The treatment with 10 μ g/mL of 5i significantly

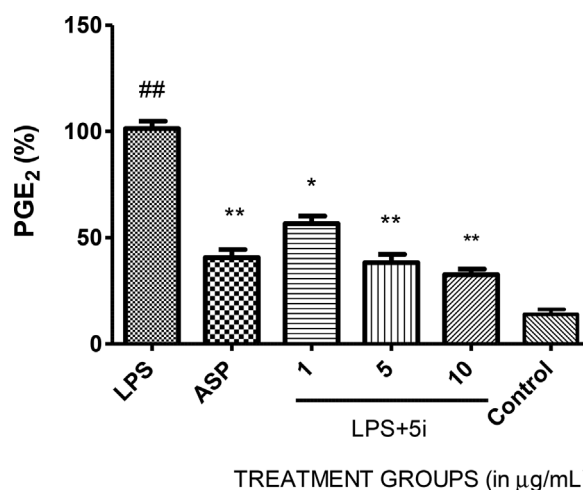


Figure 5. Effect of compound 5i on PGE₂. The values presented are mean \pm SEM. ## p < 0.01 versus control, * p < 0.05, ** p < 0.01 versus LPS.

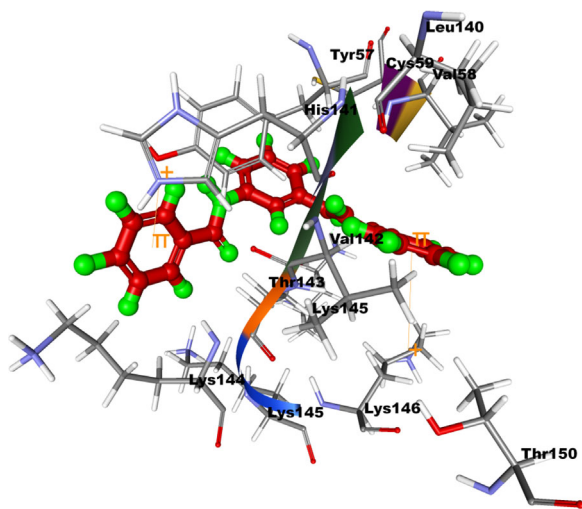


Figure 6. The orientation of compound **5i** in the active site of NF- κ B.

dwindled the level of PGE₂, which was similar to that of aspirin at 10 μ M used as a positive control in this experiment.

Docking study of compound **5i** with NF- κ B protein model

The pronounced activity of compound **5i** has prompted us to perform the molecular docking analysis to exemplify the key structural parameters necessary for this activity. For this, the NF- κ B protein model has been taken from the protein database (i.e., 1NFK.pdb) and co-crystallized ligand was removed for further processing. After that, the protein was optimized and the binding site was identified by the “binding site tool” of Discovery Studio 2.5. The legend was then allowed to dock with protein p50 NF- κ B protein with the help of CDOCKER. The procedure was followed as per the manufacturer guidelines.

Results showed that compound **5i** was efficiently docked into the active site of NF- κ B via proficient CDOCKER energy of -11.45 . As shown in Fig. 6, the compound is able to interact with Lys145, key catalytic residues via the H-bond. It will also reveal the formation of two non-bonded π -cation interaction with His141 and Lys145.

Conclusion

We have developed a series of novel chalcones derivatives via efficient synthetic methodology. The molecules were obtained in excellent yields. In antioxidant assay, these analogs showed an excellent ability to scavenge the generation of free radicals in different *in vitro* systems. Moreover, in NF- κ B assay, these molecules showed considerable inhibitory activity. Together with excellent antioxidant activity, dock score and anti-inflammatory activity via inhibition of NF- κ B, these molecules proved an excellent lead for the newer drug

discovery initiatives for the treatment of the liver cirrhotic patients.

Experimental

Chemistry

All commercially available solvents and reagents of analytical grade were used without further purification. Melting points were determined with digital thermometer and were uncorrected. FT-IR were recorded on Perkin Elmer Spectrophotometer. ¹H NMR spectra were recorded on Bruker Avance II 400 NMR and ¹³C NMR spectra on Bruker Avance II 100 NMR spectrometer in DMSO using TMS as an internal standard. Mass spectra were obtained on VG-AUTOSPEC spectrometer equipped with electrospray ionization (ESI) sources. Elemental analysis was carried out on Vario EL-III CHNOS elemental analyzer.

General procedure for the preparation N-(3-acetylphenyl)-4-fluorobenzamide (**3**)

In a 20 mL of 5% of sodium hydroxide solution taken in round bottom flask, 1-(3-amino-phenyl)ethanone **1** (1 g, 7.40 mM) was suspended. Afterwards, 2 mL 4-fluorobenzoyl chloride (**2**), 0.5 mL at a time was added to above mixture with constant shaking and vigorous stirring for 20 min. The reaction mixture was heated under reflux on water bath for 30 min until the odor of the 4-fluorobenzoyl chloride disappeared. Resultant reaction mixture was made alkaline, the solid benzoyl derivative was filtered off, and recrystallized it from petroleum ether and ethyl acetate to obtain compound **3**.

Yield: 82%; mp: 117–118°C; MW: 257.26; R_f: 0.72; FT-IR (ν_{\max} ; cm⁻¹ KBr): 3478, 3294, 3073, 2961, 1715, 1602, 1503, 1483, 1285, 1163, 1058, 842 cm⁻¹; ¹H NMR (400 MHz, DMSO, TMS) δ ppm: 8.38 (s, 1H, -NH), 8.14 (s, 1H, ArH), 8.04 (d, 1H, J=8.7 Hz, ArH), 7.63 (d, 1H, J=7.2 Hz, ArH), 7.38 (t, 1H, J=7.8 Hz, ArH), 7.94–7.83 (m, 4H, ArH), 2.58 (s, 3H, CH₃); ¹³C NMR (100 MHz, CDCl₃) δ ppm: 197.4, 166.2, 164.7, 136.9, 135.7, 133.4, 129.7, 128.9, 126.5, 124.3, 118.9, 115.2, 26.6; mass: 258.28 (M+1); elemental analysis for C₁₅H₁₂FNO₂: Calculated: C, 70.03; H, 4.70; N, 5.44. Found: C, 70.10; H, 4.69; N, 5.44.

General procedure for synthesis of substituted chalcone derivatives **5a–i**

N-(3-Acetylphenyl)-4-fluorobenzamide (**3**) (0.01 mol) and substituted benzaldehyde (**4**) (0.01 mol) were dissolved in 50 mL ethanolic solution and stirred for 30 min. It was followed by drop-wise addition of aqueous sodium hydroxide (0.05 mol) with further stirring continued for 24 h. After completion of the reaction, as monitored by TLC using the mobile phase as *n*-butanol/acetic acid/water (4:3:1), a crude product was obtained as substituted chalcone, **5(a–i)**. The resultant solid was then filtered off, washed with water, dried, and re-crystallized from ethanol.

(E)-4-Fluoro-N-(3-(3-(4-hydroxyphenyl)acryloyl)phenyl)-benzamide (5a)

Yield: 73%; mp: 215–216°C; MW: 361.37; R_f : 0.58; FT-IR (ν_{\max} ; cm^{-1} KBr): 3478, 3291, 3073, 2968, 1713, 1608, 1513, 1489, 1285, 1169, 1068, 846, 782 cm^{-1} ; ^1H NMR (400 MHz, DMSO, TMS) δ ppm: 9.15 (s, 1H, -NH), 8.14 (s, 1H, ArH), 8.11–7.42 (m, 4H, ArH), 8.06–8.02 (m, 2H, CH), 7.92 (d, 1H, $J=8.4$ Hz, ArH), 7.68 (d, 1H, $J=7.8$ Hz, ArH), 7.58 (t, 1H, $J=7.1$ Hz, ArH), 7.54–6.68 (m, 4H, ArH), 5.38 (s, 1H, Ar-OH); ^{13}C NMR (100 MHz, CDCl_3) δ ppm: 189.6, 166.3, 163.8, 157.4, 145.3, 138.8, 136.4, 133.9, 130.6, 129.9, 128.9, 127.8, 127.3, 124.5, 121.9, 118.4, 114.9, 113.7; mass: 362.41 (M+1); elemental analysis for $\text{C}_{22}\text{H}_{16}\text{FNO}_3$: Calculated: C, 73.12; H, 4.46; N, 3.88. Found: C, 73.14; H, 4.45; N, 3.91.

(E)-4-Fluoro-N-(3-(3-(3-hydroxyphenyl)acryloyl)phenyl)-benzamide (5b)

Yield: 78%; mp: 219–221°C; MW: 361.37; R_f : 0.63; FT-IR (ν_{\max} ; cm^{-1} KBr): 3482, 3295, 3073, 2971, 1712, 1608, 1509, 1482, 1287, 1172, 1064, 848, 773 cm^{-1} ; ^1H NMR (400 MHz, DMSO, TMS) δ ppm: 9.14 (s, 1H, -NH), 8.13 (s, 1H, ArH), 8.12–7.48 (m, 4H, ArH), 8.06–8.01 (m, 2H, CH), 7.89 (d, 1H, $J=8.2$ Hz, ArH), 7.63 (d, 1H, $J=7.6$ Hz, ArH), 7.56 (t, 1H, $J=6.8$ Hz, ArH), 7.53–6.64 (m, 4H, ArH), 5.39 (s, 1H, Ar-OH); ^{13}C NMR (100 MHz, CDCl_3) δ ppm: 189.4, 166.2, 164.7, 158.3, 145.1, 138.2, 136.3, 135.4, 133.7, 130.2, 129.8, 128.9, 127.4, 124.3, 121.3, 121.1, 119.5, 117.7, 115.7, 114.8; mass: 362.37 (M+1); elemental analysis for $\text{C}_{22}\text{H}_{16}\text{FNO}_3$: Calculated: C, 73.12; H, 4.46; N, 3.88. Found: C, 73.13; H, 4.48; N, 3.87.

(E)-4-Fluoro-N-(3-(3-(2-hydroxyphenyl)acryloyl)phenyl)-benzamide (5c)

Yield: 83%; mp: 223–225°C; MW: 361.37; R_f : 0.68; FT-IR (ν_{\max} ; cm^{-1} KBr): 3484, 3298, 3072, 2968, 1718, 1612, 1509, 1482, 1282, 1178, 1061, 854, 778 cm^{-1} ; ^1H NMR (400 MHz, DMSO, TMS) δ ppm: 9.17 (s, 1H, -NH), 8.15 (s, 1H, ArH), 8.30–7.42 (m, 2H, CH), 8.14–7.42 (m, 4H, ArH), 7.87 (d, 1H, $J=8.4$ Hz, ArH), 7.63 (d, 1H, $J=7.6$ Hz, ArH), 7.58 (t, 1H, $J=6.9$ Hz, ArH), 7.60–6.48 (m, 4H, ArH), 5.42 (s, 1H, Ar-OH); ^{13}C NMR (100 MHz, CDCl_3) δ ppm: 189.1, 166.3, 164.8, 158.4, 145.3, 138.7, 136.4, 135.7, 133.7, 130.1, 129.9, 128.3, 127.4, 124.1, 121.5, 121.3, 119.8, 117.6, 115.8, 114.9; mass: 362.45 (M+1); elemental analysis for $\text{C}_{22}\text{H}_{16}\text{FNO}_3$: Calculated: C, 73.12; H, 4.46; N, 3.88. Found: C, 73.15; H, 4.45; N, 3.91.

(E)-4-Fluoro-N-(3-(3-(4-methoxyphenyl)acryloyl)phenyl)-benzamide (5d)

Yield: 68%; mp: 233–234°C; MW: 375.39; R_f : 0.74; FT-IR (ν_{\max} ; cm^{-1} KBr): 3492, 3289, 3078, 2972, 1713, 1618, 1513, 1482, 1287, 1172, 1068, 851, 772 cm^{-1} ; ^1H NMR (400 MHz, DMSO, TMS) δ ppm: 9.15 (s, 1H, -NH), 8.14 (s, 1H, ArH), 8.06–8.02 (m, 2H, CH), 8.14–7.48 (m, 4H, ArH), 7.89 (d, 1H, $J=8.4$ Hz, ArH), 7.64 (d, 1H, $J=7.5$ Hz, ArH), 7.62 (t, 1H, $J=6.3$ Hz, ArH), 7.62–6.94 (m, 4H, ArH), 3.82 (s, 3H, Ar-OCH₃); ^{13}C NMR (100 MHz, CDCl_3) δ ppm: 189.7, 166.2, 164.7, 159.8, 145.1, 138.2, 136.4, 133.5, 130.7, 129.8, 129.2, 127.5, 127.1, 124.3, 121.1, 119.5,

115.6, 114.2, 55.7; mass: 376.42 (M+1); elemental analysis for $\text{C}_{23}\text{H}_{18}\text{FNO}_3$: Calculated: C, 73.59; H, 4.83; N, 3.73. Found: C, 73.61; H, 4.84; N, 3.75.

(E)-4-Fluoro-N-(3-(3-(3-methoxyphenyl)acryloyl)phenyl)-benzamide (5e)

Yield: 72%; mp: 238–239°C; MW: 375.39; R_f : 0.71; FT-IR (ν_{\max} ; cm^{-1} KBr): 3490, 3287, 3072, 2978, 1717, 1609, 1518, 1487, 1282, 1178, 1072, 859, 778 cm^{-1} ; ^1H NMR (400 MHz, DMSO, TMS) δ ppm: 9.15 (s, 1H, -NH), 8.12 (s, 1H, ArH), 8.05–8.03 (m, 2H, CH), 8.12–7.42 (m, 4H, ArH), 7.89 (d, 1H, $J=8.4$ Hz, ArH), 7.63 (d, 1H, $J=7.3$ Hz, ArH), 7.59–6.87 (m, 4H, ArH), 7.60 (t, 1H, $J=6.5$ Hz, ArH), 3.87 (s, 3H, Ar-OCH₃); ^{13}C NMR (100 MHz, CDCl_3) δ ppm: 189.5, 166.3, 164.8, 160.5, 145.2, 138.1, 136.4, 135.1, 133.7, 129.7, 129.1, 128.5, 127.4, 127.1, 124.3, 121.3, 120.8, 119.3, 115.2, 113.5, 55.8; mass: 376.45 (M+1); elemental analysis for $\text{C}_{23}\text{H}_{18}\text{FNO}_3$: Calculated: C, 73.59; H, 4.83; N, 3.73. Found: C, 73.58; H, 4.86; N, 3.72.

(E)-4-Fluoro-N-(3-(3-(2-methoxyphenyl)acryloyl)phenyl)-benzamide (5f)

Yield: 79%; mp: 241–242°C; MW: 375.39; R_f : 0.63; FT-IR (ν_{\max} ; cm^{-1} KBr): 3495, 3282, 3078, 2985, 1709, 1612, 1509, 1487, 1287, 1171, 1076, 863, 787 cm^{-1} ; ^1H NMR (400 MHz, DMSO, TMS) δ ppm: 9.14 (s, 1H, -NH), 8.13 (s, 1H, ArH), 8.33–7.43 (m, 2H, CH), 8.12–7.48 (m, 4H, ArH), 7.89 (d, 1H, $J=8.4$ Hz, ArH), 7.63 (d, 1H, $J=7.3$ Hz, ArH), 7.66–6.94 (m, 4H, ArH), 7.62 (t, 1H, $J=6.4$ Hz, ArH), 3.84 (s, 3H, Ar-OCH₃); ^{13}C NMR (100 MHz, CDCl_3) δ ppm: 189.3, 166.5, 164.7, 159.2, 141.5, 138.3, 137.8, 135.2, 133.7, 129.8, 129.2, 128.9, 127.5, 125.7, 124.1, 121.5, 120.9, 119.5, 115.6, 114.2, 56.2; mass: 376.42 (M+1); elemental analysis for $\text{C}_{23}\text{H}_{18}\text{FNO}_3$: Calculated: C, 73.59; H, 4.83; N, 3.73. Found: C, 73.62; H, 4.84; N, 3.75.

(E)-N-(3-(3-(4-Chlorophenyl)acryloyl)phenyl)-4-fluorobenzamide (5g)

Yield: 62%; mp: 268–269°C; MW: 379.81; R_f : 0.87; FT-IR (ν_{\max} ; cm^{-1} KBr): 3491, 3283, 3072, 2987, 1712, 1609, 1516, 1493, 1287, 1178, 1094, 868, 781 cm^{-1} ; ^1H NMR (400 MHz, DMSO, TMS) δ ppm: 9.15 (s, 1H, -NH), 8.12 (s, 1H, ArH), 8.13–7.48 (m, 4H, ArH), 8.06–7.62 (m, 2H, CH), 7.88 (d, 1H, $J=8.4$ Hz, ArH), 7.64 (d, 1H, $J=7.6$ Hz, ArH), 7.61 (t, 1H, $J=6.5$ Hz, ArH), 7.68–7.46 (m, 4H, ArH); ^{13}C NMR (100 MHz, CDCl_3) δ ppm: 189.5, 166.3, 164.7, 145.2, 138.3, 136.1, 133.5, 133.7, 133.1, 129.8, 129.1, 128.9, 128.5, 127.4, 124.1, 121.7, 119.8, 115.6; mass: 380.85 (M+1); elemental analysis for $\text{C}_{22}\text{H}_{15}\text{ClFNO}_2$: Calculated: C, 69.57; H, 3.98; N, 3.69. Found: C, 68.58; H, 3.97; N, 3.71.

(E)-N-(3-(3-(4-Bromophenyl)acryloyl)phenyl)-4-fluorobenzamide (5h)

Yield: 65%; mp: 282–283°C; MW: 424.26; R_f : 0.78; FT-IR (ν_{\max} ; cm^{-1} KBr): 3489, 3291, 3076, 2983, 1709, 1618, 1502, 1498, 1282, 1175, 1094, 875, 789 cm^{-1} ; ^1H NMR (400 MHz, DMSO, TMS) δ ppm: 9.15 (s, 1H, -NH), 8.13 (s, 1H, ArH), 8.12–7.42 (m, 4H, ArH), 8.06–7.61 (m, 2H, CH), 7.89 (d, 1H, $J=8.2$ Hz, ArH),

7.64 (d, 1H, $J = 7.6$ Hz, ArH), 7.61 (t, 1H, $J = 6.5$ Hz, ArH), 7.61–7.58 (m, 4H, ArH); ^{13}C NMR (100 MHz, CDCl_3) δ ppm: 189.4, 166.3, 164.5, 145.1, 138.2, 136.3, 134.2, 133.8, 131.5, 129.7, 129.3, 128.6, 127.4, 124.1, 122.3, 121.3, 119.5, 115.8; mass: 424.28 (M+1); elemental analysis for $\text{C}_{22}\text{H}_{15}\text{BrFNO}_2$: Calculated: C, 62.28; H, 3.56; N, 3.30. Found: C, 62.31; H, 3.57; N, 3.28.

(E)-4-Fluoro-N-(3-(3-(4-fluorophenyl)acryloyl)phenyl)benzamide (5i)

Yield: 76%; mp: 273–275°C; MW: 363.36; R_f : 0.71; FT-IR (ν_{max} ; cm^{-1} KBr): 3498, 3282, 3066, 2989, 1718, 1612, 1509, 1489, 1287, 1175, 1098, 876, 792 cm^{-1} ; ^1H NMR (400 MHz, DMSO, TMS) δ ppm: 9.15 (s, 1H, –NH), 8.13 (s, 1H, ArH), 8.12–7.44 (m, 4H, ArH), 8.06–7.58 (m, 2H, CH), 7.87 (d, 1H, $J = 8.4$ Hz, ArH), 7.64 (d, 1H, $J = 7.6$ Hz, ArH), 7.61 (t, 1H, $J = 6.5$ Hz, ArH), 7.72–7.19 (m, 4H, ArH); ^{13}C NMR (100 MHz, CDCl_3) δ ppm: 189.5, 166.4, 164.7, 162.3, 145.3, 138.1, 136.4, 133.5, 130.8, 130.2, 129.8, 129.2, 127.4, 124.1, 121.5, 119.5, 115.6, 114.9; mass: 364.38 (M+1); elemental analysis for $\text{C}_{22}\text{H}_{15}\text{F}_2\text{NO}_2$: Calculated: C, 72.72; H, 4.16; N, 3.85. Found: C, 72.71; H, 4.18; N, 3.82.

Antioxidant activity [17]

Hydrogen peroxide (H_2O_2) scavenging activity

Phosphate buffer (pH 7.4) was taken for preparing a solution of H_2O_2 (40 mM), which was used to conduct this experiment. The 1 mM concentrations of various target compounds were added to the above prepared H_2O_2 solution (0.6 mL, 40 mM). After 10 min, the absorbance of H_2O_2 at 230 nm was determined against a blank solution containing phosphate buffer without drug. The percentage scavenging of hydrogen peroxide of synthetic compounds and standard compounds was calculated using the following formula:

$$\text{Percentage scavenged } [\text{H}_2\text{O}_2] = \left[\frac{(A_0 - A_1)}{A_0} \right] \times 100$$

where A_0 is the absorbance of the control and A_1 is the absorbance in the presence of the sample of MO and standards.

DPPH radical scavenging activity

In this method, briefly, 1 mL of synthesized compounds as 100 mM was mixed with 3.0 mL DPPH (0.5 mmol/L in methanol); the resultant absorbance was recorded at 517 nm after 30 min of incubation at 37°C. Following formula was used to assess the percentage of scavenging activity of the target compounds:

$$\text{Percentage of inhibition} = \left[\frac{(A_{\text{control}} - A_{\text{sample}})}{A_{\text{control}}} \right] \times 100$$

where A_{control} is the absorbance of DPPH and A_{sample} is the absorbance of the reaction mixture (DPPH with sample).

Ferrous reducing power

According to the previous procedure, 100 mM of the synthesized compounds (1.0 mL) was mixed with 2.5 mL of phosphate buffer (0.2 M, pH 6.6) and 2.5 mL of potassium ferricyanide (1%). The resulting mixture was incubated at 50°C for 20 min with TCA (10%: 2.5 mL). Then the mixture was centrifuged at 3000 rpm for 10 min. The resulting supernatant (2.5 mL) was mixed with 2.5 mL of distilled water and 0.5 mL of ferric chloride (1%) and the absorbance was measured at 700 nm. Higher absorbance of the reaction mixture indicated greater reducing power. Thus, the reducing power of compounds was compared with that of standard antioxidant.

Nitric oxide radical scavenging activity

Nitric oxide radicals were generated from sodium nitroprusside solution. One milliliter of 10 mM sodium nitroprusside was mixed with 1 mL of 100 mM target compounds in phosphate buffer (0.2 M, pH 7.4). The mixture was incubated at 25°C for 150 min. After incubation, the reaction mixture was mixed with 1.0 mL of pre-prepared Griess reagent (1% sulphanilamide, 0.1% naphthyl ethylenediamine dichloride, and 2% phosphoric acid). The absorbance was measured at 546 nm and percentage of inhibition was calculated using the same formula as given below. The decreasing absorbance indicates a high nitric oxide scavenging activity.

$$\text{Percentage of inhibition} = \left[\frac{(A_{\text{control}} - A_{\text{sample}})}{A_{\text{control}}} \right] \times 100$$

where A_{control} is the absorbance of nitric oxide and A_{sample} is the absorbance of the reaction mixture (nitric oxide with sample).

NF- κ B inhibition assay

RAW264.7 macrophages were purchased from American Type Culture Collection (ATCC, USA). Cells were cultured in DMEM with 10% FBS, 100 mg/mL streptomycin, and 100 U/mL penicillin in humidified 5% CO_2 at 37°C. The 80% confluency of RAW264.7 cells was achieved in six-well plates and transfected with 1 μg of the NF- κ B reporter construct, along with 0.5 μg of pSVGal plasmid using LipofectAMINE 2000 (Invitrogen) in Opti-MEM medium (Gibco). After 24 h of transfection, cells were treated with LPS or target derivatives (100 μM) for an additional 2 h, and then lysed using the reporter lysis buffer (Promega). Luciferase assays were performed using 20 mL of cell extract and 100 mL of luciferin substrate (Promega), and the luciferase activity was measured using a Dual-Luciferase Reporter Assay System (Promega) according to the manufacturer's instructions. Data are normalized for transfection efficiency by dividing firefly luciferase activity with that of Renilla luciferase.

Cell viability assay

The MTT (3-(4,5-dimethyl-2-yl)-2,5-diphenyltetrazolium bromide) assay was used to assess the cytotoxic level of compound 5i on RAW264.7 cells. The cells were grown in

96-well plates at a density of 5×10^3 cells/well. After 24 h, the cells in the culture wells were re-freshed with fresh medium and were treated with different concentrations of **5i**. After 48 h of incubation, cells were rewashed and 20 μ L of MTT (5 mg/mL) was added and incubated for 4 h. Finally, DMSO (150 μ L) was added to solubilize the formazan salt formed and the amount of formazan salt was determined by measuring the OD at 540 nm using an GENios[®] microplate reader (Tecan Austria GmbH, Groedig, Austria). Relative cell viability was determined by the amount of MTT converted into formazan salt. Viability of cells was quantified as a percentage compared to the control (OD of treated cells – OD of blank/OD of control – OD of blank \times 100) and dose–response curves were developed. The data were expressed as mean from at least three independent experiments and $p < 0.05$ was considered significant.

Immunoassays

Enzyme immunoassay of TNF- α , IL-1 β , and IL-6

Inflammatory mediators such as TNF- α , IL-1 β , and IL-6 were measured by solid phase sandwich enzyme-linked immunosorbent assay (ELISA) according to the manufacturer's protocol (Code RPN 2751, RPN 2718, and RPN 2708, Amersham Pharmacia Biosciences, Piscataway, NJ, USA) without prior extraction or purification. Standard curves from 10.24–400, 50–2450, and 51–2000 pg/mL were used in order to evaluate the concentrations of TNF- α , IL-1 β , and IL-6, respectively. Results were calculated by using nonlinear regression of a four parameter logistic model.

Enzyme immunoassay of PGE₂

PGE₂ was measured by enzyme immunoassay without prior extraction or purification according to the manufacturer's protocol (Code RPN 222, Amersham Pharmacia Biosciences, Piscataway, NJ, USA). A concentration range of 2.5–320 pg/well was used to construct the standard curve. PGE₂ concentrations in the samples were calculated by using nonlinear regression of a four parameter logistic model.

Docking study

CDOCKER is a grid-based molecular docking method that works on CHARMM force fields. During docking process, the protein was firstly held rigid and the ligand was allowed to freely rotate. Two hundred random ligand conformations were then generated from the initial ligand through a series of process including high temperature molecular dynamics, followed by random rotations; refinement by grid-based (GRID 1) simulated annealing, and a final grid-based or full force field minimization. In this experiment, the target ligand was heated to a temperature of 700 K in 2000 steps. The cooling of 5000 steps was performed with 300 K cooling temperature, while the extension of grid extension was set to 10 Å. Moreover, the hydrogen atoms were added to the

structure and all ionizable residues were set at their default protonation state at a neutral pH. For ligand **6e**, 10 ligand binding poses were ranked according to their CDOCKER energies, and the predicted binding interactions were analyzed. In last, the best 10 ligand binding poses were chosen and carried out *in situ* ligand minimization using standard protocol.

Statistical analysis

Statistical analyses were performed using ANOVA followed by the Bonferroni *t*-test for multigroup comparisons; $p < 0.05$ was considered significant for all tests. Data are expressed as mean \pm standard deviation. The statistical analysis was carried out with the help of GraphPad Prism 5 Software.

The authors have declared no conflicts of interest.

References

- [1] L. Rui, *Compr. Physiol.* **2014**, *4*, 177–197.
- [2] J. P. Iredale, *J. Clin. Invest.* **2007**, *117*, 539–548.
- [3] S. L. Friedman, *Gastroenterology* **2008**, *134*, 1655–1669.
- [4] E. Novo, S. Cannito, C. Paternostro, C. Bocca, A. Miglietta, M. Parola, *Arch. Biochem. Biophys.* **2014**, *548*, 20–37.
- [5] G. Bjelakovic, L. L. Gluud, D. Nikolova, M. Bjelakovic, A. Nagorni, C. Gluud, *Cochrane Libr.* **2011**, *3*(16), D007749.
- [6] E. Liaskou, D. V. Wilson, Y. H. Oo, *Mediat. Inflamm.* **2012**, *21*, 949157.
- [7] T. Luedde, F. Robert, *Nat. Rev. Gastroenterol. Hepatol.* **2011**, *8*, 108–118.
- [8] A. Oeckinghaus, S. Ghosh, *Cold Spring Harb. Perspect. Biol.* **2009**, *1*, a000034.
- [9] Claisen-Schmidt Condensation **2010**, *145*, 660–664.
- [10] G. Achanta, A. Modzelewska, L. Feng, S. R. Khan, P. Huang, *Mol. Pharmacol.* **2006**, *70*, 426–433.
- [11] T. D. Tran, T. T. Nguyen, T. H. Do, T. N. Huynh, C. D. Tran, K. M. Thai, *Molecules* **2012**, *17*, 6684–6696.
- [12] K. L. Lahtchev, D. I. Batovska, S. P. Parushev, V. M. Ubiyovkov, A. A. Sibirny, *Eur. J. Med. Chem.* **2008**, *43*, 2220–2228.
- [13] S. U. F. Rizvi, H. L. Siddiqui, M. Johns, M. Detorio, R. F. Schinazi, *Med. Chem. Res.* **2012**, *21*, 3741–3749.
- [14] N. Yadav, S. K. Dixit, A. Bhattacharya, L. C. Mishra, M. Sharma, S. K. Awasthi, V. K. Bhasin, *Chem. Biol. Drug Des.* **2012**, *80*, 340–347.
- [15] M. R. El Sayed Aly, H. H. Abd El Razek Fodah, S. Y. Saleh, *Eur. J. Med. Chem.* **2014**, *76*, 517–530.
- [16] N. Mateeva, M. Gangapuram, E. Mazziio, S. Eyunni, K. F. Soliman, K. K. Redda, *Med. Chem. Res.* **2015**, *24*, 1672–1680.
- [17] H. K. Sharma, A. Kumar, *Asian J. Chem.* **2011**, *23*, 434–438.